

Article

Nanoporous Silica-Dye Microspheres for Enhanced Colorimetric Detection of Cyclohexanone

Zheng Li 

Department of Chemical and Biomolecular Engineering, North Carolina State University, 911 Partner Way, Campus Box 7905, Raleigh, NC 27695, USA; zli47@ncsu.edu; Tel.: +1-217-418-9162

Received: 18 July 2018; Accepted: 7 August 2018; Published: 13 August 2018



Abstract: Forensic detection of non-volatile nitro explosives poses a difficult analytical challenge. A colorimetric sensor comprising of ultrasonically prepared silica-dye microspheres was developed for the sensitive gas detection of cyclohexanone, a volatile marker of explosives 1,3,5-trinitro-1,3,5-triazinane (RDX) and 1,3,5,7-tetranitro-1,3,5,7-tetrazocane (HMX). The silica-dye composites were synthesized from the hydrolysis of ultrasonically sprayed organosiloxanes under mild heating conditions (150 °C), which yielded microspherical, nanoporous structures with high surface area (~300 m²/g) for gas exposure. The sensor inks were deposited on cellulose paper and given sensitive colorimetric responses to trace the amount of cyclohexanone vapors even at sub-ppm levels, with a detection limit down to ~150 ppb. The sensor showed high chemical specificity towards cyclohexanone against humidity and other classes of common solvents, including ethanol, acetonitrile, ether, ethyl acetate, and ammonia. Paper-based colorimetric sensors with hierarchical nanostructures could represent an alternative sensing material for practical applications in the detection of explosives.

Keywords: silica-dye microspheres; hierarchical nanostructure; colorimetric sensing; gaseous cyclohexanone; ppb detection; explosive screening

1. Introduction

Today, there still remains a difficult scientific challenge in the accurate detection and identification of explosives and chemical or biological agents at trace amounts [1]. Sensitivity, specificity, reproducibility, ease of handling, environmental tolerance, and cost are all important factors that ought to be taken into account in the development of useful gas detectors for explosives [2]. Among many energetic materials, 1,3,5-trinitro-1,3,5-triazinane (RDX) and 1,3,5,7-tetranitro-1,3,5,7-tetrazocane (HMX) are two typical nitro-explosives that are widely used by terrorists and, therefore, pose a great threat to civilian and military security [3,4]. However, it is rather difficult to detect either RDX or HMX in the gas phase due to its extremely low volatility, with a saturated vapor pressure of only 10 ppt at ambient conditions. An alternative approach for the indirect identification of nitro explosives is to target more volatile, but non-energetic, species, introduced during their manufacturing, e.g., cyclohexanone, a common solvent used for the recrystallization of RDX or HMX [5,6]. Cyclohexanone has a significantly high vapor pressure of ~6500 ppm at 20 °C, thus, it is well-suited to act as a vapor signature for explosive sensing.

In the past decade, a large number of analytical methods for trace explosive screening have been investigated, including gas chromatography-mass spectrometry (GC-MS) [7–10], electronic noses [11–14], ion mobility spectrometry [5,15–18], surface acoustic wave devices [19–21] and fluorimetry [22–25]. Some effective approaches, such as solid-phase microextraction (SPME) [26–28], have been extensively explored for ultrasensitive gaseous detection of non-volatile explosives at the ppb or ppt level. Many of those techniques, however, suffer from at least one of the following drawbacks:

Lack of portability, time-consuming sample preparation, demands in sophisticated instrumentation or highly trained personnel for operation and data acquisition [28,29].

I described in this work a new method that encapsulates a ketone-sensitive colorimetric indicator, pararosaniline, in the recently reported silica microspheres [30] for the sensitive detection of trace levels of cyclohexanone vapors. The sensor materials were made from the hydrolysis of siloxane monomers under mild heating and ultrasonic conditions, which lead to the formation of nanoporous, organically modified silica microspheres, with an average diameter of ~500 nm. The as-synthesized inks were pin-printed on the cellulose paper and solidified with the evaporation of solvents prior to the measurements on an ordinary flatbed scanner. The silica-dye composite sensor is optically responsive to cyclohexanone but insensitive to humidity or other common solvents found in explosives including ethanol, acetonitrile, ether, ammonia and ethyl acetate. The sensors show greatly improved sensitivity to cyclohexanone that can reach as low as ~150 ppb, four times higher than those made from the bulk plasticized films or amorphous sol–gel suspensions. This ultrasonic synthesis provided a scalable and continuous approach for the preparation of porous materials with hierarchical nanostructures for gas sensing applications.

2. Experimental Methods

2.1. Reagents and Materials

All chemical reagents, including tetraethoxysilane (TEOS), ethyltriethoxysilane (ETES), pararosaniline, hydrochloric acid, ethanol, polyethylene glycol and other solvents, were analytical-reagent grade and used as received unless otherwise specified.

2.2. Preparation of Silica-Dye Composite Microspheres

The synthesis of silica-dye composite microspheres, using a continuous ultrasonic setup, is shown in Figure 1; TEOS (0.01 mol) and ethyltriethoxysilanes (0.02 mol) were mixed with ethanol (13 mL), nanopure water (26 mL), and aqueous HCl (1 mL, 0.1 M) plus the ketone-responsive indicator, pararosaniline (100 mg). The precursor solution was introduced into a glass cell and nebulized by a home-made ultrasonic humidifier working at ~10 W/cm². The resulting aerosol was carried by an N₂ gas through a tube furnace at a mild heating temperature of 150–300 °C to ensure the optimal porosity of the microspheres; the N₂ gas flow was set at 1.0 SLPM (standard liters per minute). The product was collected in a couple of connected bubblers containing a 1:1 *v/v* mixture of nanopure water and ethanol, then it was centrifuged and washed with the same solvents three times to remove uncaptured indicators. The final product was redispersed in 9:1 mixture of ethanol and polyethylene glycol (Mw ≈ 10,000) prior to sensor printing.

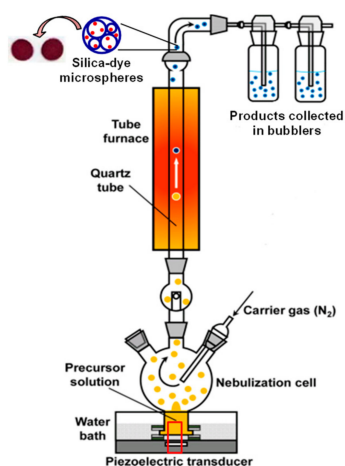


Figure 1. Ultrasonic spray synthesis of the porous silica-dye composite microspheres.

2.3. Material Characterization

For characterization of silica-dye microspheres, powder X-ray diffraction (XRD) patterns were obtained on a Siemens–Bruker (Billerica, MA, USA) D-5000 XRD instrument, using Cu K α radiation (wavelength 1.5418 Å) operated at 40 kV and 30 mA. SEM was carried out using a Hitachi (Chiyoda, Tokyo, Japan) S-4700 operated at 10 kV. Transmission electron microscopy (TEM) was performed using a JEOL (Akishima, Tokyo, Japan) 2000FX with an acceleration voltage of 200 kV. The Brunauer–Emmett–Teller (BET) specific surface areas were measured by a Quantachrome (Anton Paar, Graz, Austria) NOVA 2200e system.

2.4. Preparation of the Paper-Based Sensor

The colorimetric sensor was deposited on nitrocellulose paper (Whatman, Maidstone, UK) with a robotic pin printer, as described in details in previous literature [31–33], which delivered nanoporous inks with silica-dye microspheres encapsulating a ketone-responsive indicator, pararosaniline. After printing, the sensor was dried under vacuum for 1 h at room temperature and stored in an N₂ atmosphere for at least 24 h before any measurements were taken.

2.5. Measurement of Gaseous Cyclohexanone

Analyte flow streams were produced by bubbling dry N₂ through the liquid cyclohexanone. The resulting saturated vapors were then mixed with a diluting stream of dry and wet N₂ to attain the desired concentrations between 0.1 and 100 ppm, at 50% relative humidity (RH), using MKS (Andover, MA, USA) digital mass flow controllers (MFCs). The flow rate was kept at 0.5 SLPM for all the experiments performed in this work. Sensor responses were collected on an Epson (Suwa, Nagano Prefecture, Japan) Perfection V600 flatbed scanner; sensors were equilibrated with 50% RH nitrogen for 1 min to capture the before-exposure image. The after-exposure image was acquired after 2 min of exposure to cyclohexanone vapor.

2.6. Data Analysis

Colorimetric response of each sensor element was calculated from the differences in red, green, and blue (Δ RGB) values by comparing before and after exposure images using the online software ImageJ. For visualization purposes only, color difference RGB values were expanded from 3 bits (i.e., 3–10) to 8 bits (i.e., 0–255). For the measurement of the control of each concentration of cyclohexanone, quintuplicate trials were collected. Signal-to-noise ratio (S/N) was calculated from the Euclidean distance (ED, i.e., the square root of the sum of square of RGB channels) and incorporated in the final database for statistical analysis. For this, the signals were defined as the difference between the response of a certain concentration of cyclohexanone and that of the averaged control, and noise was defined as the standard deviation among quintuplicate trials of the control for ED of each spot, namely Equations (1) and (2):

$$S = ED_{\text{cyclohexanone}-k} - ED_{\text{control-avg}} \quad (1)$$

$$N = \sum_{k=1}^n \left(ED_{\text{control}-k} - ED_{\text{control-avg}} \right)^2 / (n - 1) \quad (2)$$

3. Results and Discussions

3.1. Silica-Dye Composite Microspheres

Factors that reflect the performance of optical gas sensors, such as response time, sensitivity, reproducibility, selectivity, susceptibility to interferents, can be heavily influenced by the choice of substrates or matrices of the colorants [34–36]. Porous organosilica materials [37–40] provide impressive physical and chemical properties including high stability, tunable porosity or hydrophobicity, and ease of modification, which can be selected as sensor media to ensure the

robust encapsulation and solvation of chemical dyes, a high contact area for gas exposure, as well as prevention of dye leaching. Porous silica matrices, as host materials, can impressively enhance overall sensitivity of chemo-responsive dyes for gaseous or aqueous detection of relevant analytes of interest.

Ultrasonic spray pyrolysis (USP) [41–43] is a tunable and scalable approach for the preparation of a wide variety of hierarchical materials, including porous carbons, transition metal oxides or chalcogenides, metallic nanoparticles, and polymers, among others. USP is also well suited for the continuous synthesis of organosilica particles, mostly those with micro-spherical geometries. In a typical USP process, ultrasound is used to nebulize the precursor solution droplets which are dispersed in an inert carrier gas (Ar or N₂, Figure 1). With the pyrolysis of aerosol droplets in the furnace, an evaporation of solvents and reactions between precursors occur, to generate microscale or nanoscale solid products with spherical morphologies. Using low-volatility precursors, the reactions responsible for the formation of products are confined within each individual droplet. The droplets formed in this matter can serve as individual chemical microreactors that impose morphology control on the products.

Choices of siloxane precursors and reaction temperatures used in ultrasonic synthesis can largely affect the morphology of microspheres [44,45]. To that end, a mixture of TEOS and ETES (1:2 molar ratio) was employed as the precursor to guarantee the optimal permeability and porosity of the as-synthesized silica-dye composites. A ketone-responsive indicator, pararosaniline, was incorporated in the precursor for the ultrasonic spray synthesis. The aerosol-gel reaction was kept at either 150 °C or 300 °C to investigate the impact of the temperature on morphologies of the products. Electron microscopy graphs reveal that hollow and more porous microspheres (520 ± 50 nm in diameter), with smoother surfaces, were obtained at 150 °C (Figure 2a), while those micron-scale particles tended to become more solid and compact (440 ± 60 nm in diameter) as the temperature went up to 300 °C (Figure 2b). Powder XRD spectrum shows an amorphous polymeric structure of both microspheres, as indicated by the characteristic broad peaks at 25° and 40° (Figure S1).

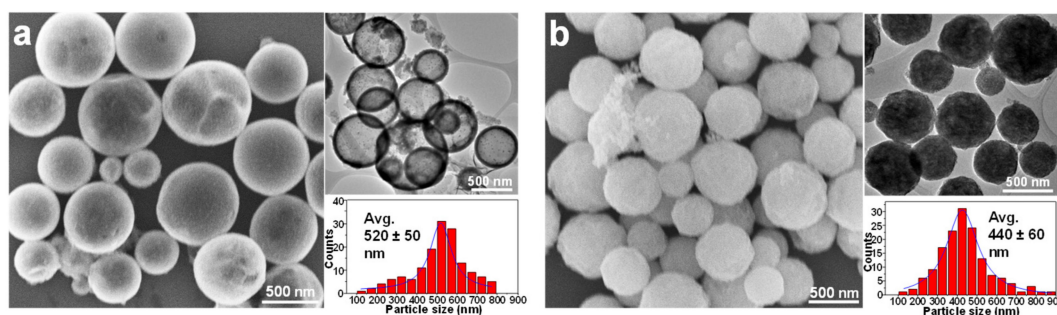


Figure 2. Morphologies of Silica-dye microspheres synthesized at (a) 150 °C and (b) 300 °C, with the particle size of 520 ± 50 nm and 440 ± 60 nm, respectively.

3.2. Sensor Responses of Gaseous Cyclohexanone

Colorimetric inks made of silica-dye microspheres were pin-printed on a nitrocellulose paper and dried out for the detection of target vapors, which was generated from the saturated vapor of liquid cyclohexanone. The designed sensing mechanism was based on nucleophilic addition by the three equivalent amino groups of the dye to the carbonyl moiety of cyclohexanone in the formation of an imine species [46–49], leading to changes in the UV-vis absorption band that allows for the direct identification of low or high concentration by the naked eye (Figure 3).

The colorimetric reactions of typical indicators with gas analytes, using porous matrices, have been proven in previous research to be able to reach equilibrated responses within 1 or 2 min [33,50]. The sensor element essentially has a fast response time (i.e., reaching 50% of saturated response in the first 30 s of exposure) and once equilibrated, the overall response is independent of flow rates or doses. Therefore, I collected sensor responses for different concentrations of cyclohexanone after 2 min of exposure, as shown in Figure 4. Significant color changes from red (color of the initial dye) to dark red

(color of the product after exposure) were observed for the target molecule at ppm and even sub-ppm levels. Sensor responses became rather strong at gas concentrations above 1 ppm, while slight color changes could still be discerned in the range of 0.1–0.25 ppm. The left sensor element, made from 150 °C silica microsphere suspensions, was generally more reactive than the right one, prepared at 300 °C for each concentration, which is consistent with the magnitude of the surface areas of the two nanoporous inks: Silica microspheres synthesized at 150 or 300 °C give BET specific surface areas of 288 or 179 m²/g, respectively (Figure 5a,b); the higher surface area for the 150 °C silica microsphere facilitates the gas exposure of dye molecules, and, therefore, results in an enhanced responsiveness to the carbonyl compound.

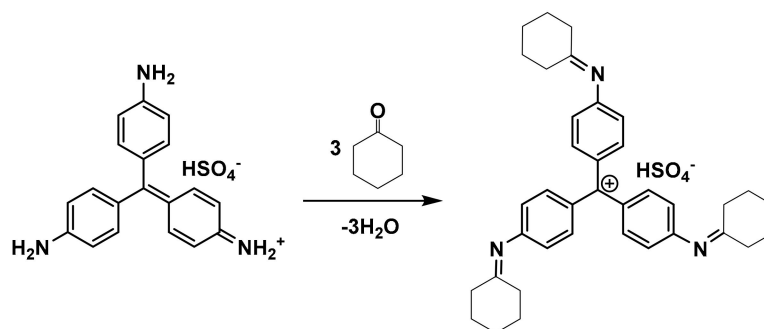


Figure 3. Colorimetric detection mechanism of cyclohexanone using an amine-based indicator, pararosaniline, in the formation of an imine product.

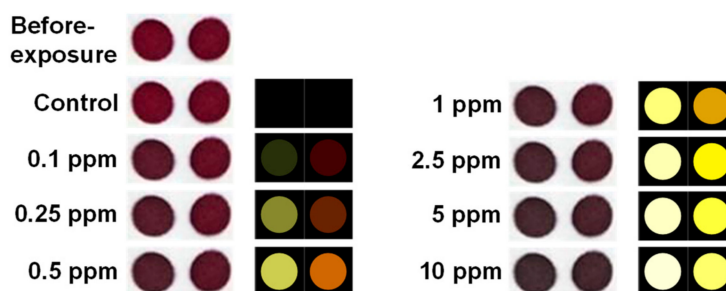


Figure 4. Images of sensors made from 150 (left spot of each sensor strip image) and 300 °C (right spot) microspheres before and after the vapor exposure, and RGB color different profiles (right) that show colorimetric sensor responses to different concentrations of cyclohexanone plus a control (i.e., N₂) for 2 min. Each pattern was averaged out of three trials. For display purposes, each RGB profile was narrowed down from 8 bit (0–255) to 3 bit (3–10) color range.

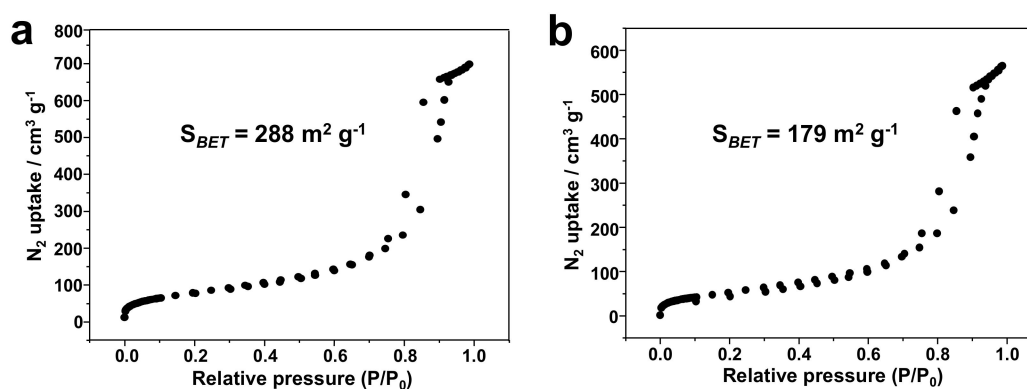


Figure 5. Cont.

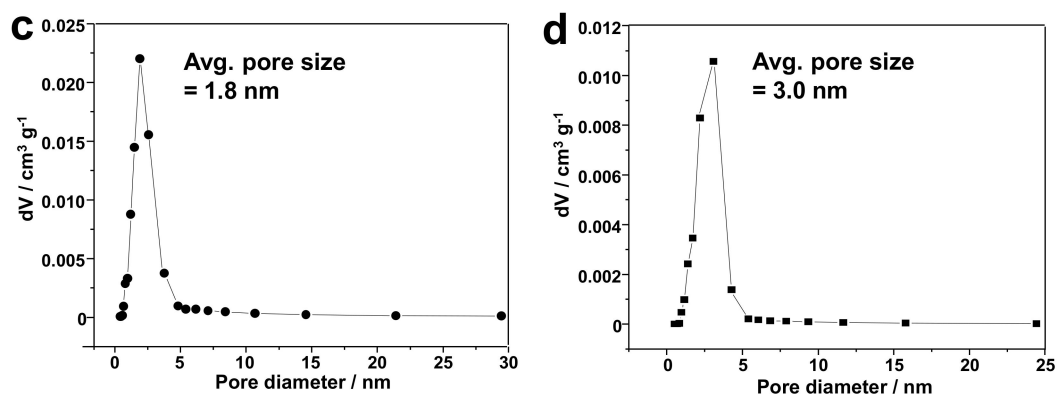


Figure 5. Gas adsorption experiments of two microspheres. (a,b), N_2 adsorption isotherms of two microspheres prepared at 150 and 300 °C, respectively; (c,d), pore size distributions of two microspheres based on Barrett-Joyner-Halenda (BJH) model. All measurements were performed with N_2 at 78 K.

3.3. Discussions: Influence of Nanostructure on Sensing Properties

The development of chemical sensing platforms has increasingly employed substrates that are fabricated with advanced processing techniques; their overall morphologies, especially some microstructures or nanostructures, must be fully characterized in order to gain a comprehensive insight into the sensing mechanisms. The high-resolution TEM (HR-TEM) micrographs demonstrate the highly hierarchical structure of the microspheres synthesized at 150 °C, from which a substantial number of nanopores can be observed that are incorporated in the microsphere (1–2 nm in diameter, Figure 6a). The hierarchically nanoscale features of the microsphere contribute to their improved surface area and resulting enhanced gas sensing properties. However, materials obtained at higher temperature show no significant nanopores, which results in reduced porosity and reactivity to gaseous analytes (Figure 6b). This observation is consistent with the pore size distributions of both microspheres, according to the Barrett-Joyner-Halenda (BJH) model [51] (Figure 5c,d).

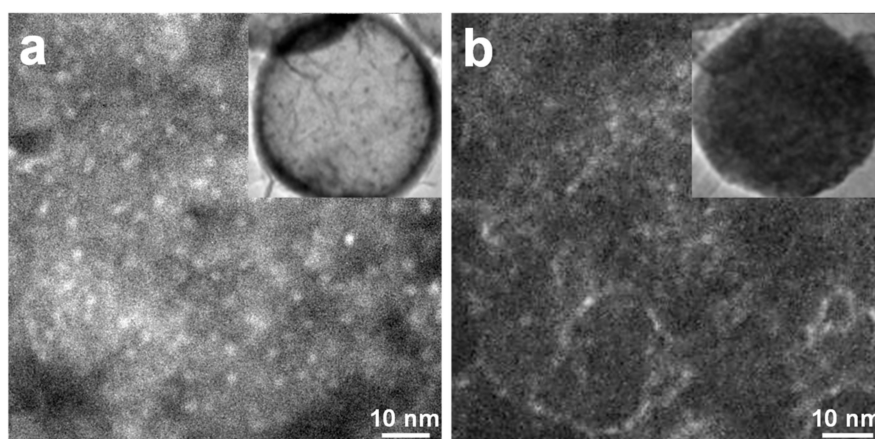


Figure 6. High resolution transmission electron microscope (HR-TEM) micrographs of microspheres synthesized at (a) 150 °C and (b) 300 °C. Hierarchical structure with nanopores is present in graph (a).

The porosity of any sensing materials has profound impacts on both the accessibility of analyte molecules to receptors and the ability to immobilize or encapsulate chemical dyes. Based on the appearance of materials obtained under different synthetic conditions, a mechanism for the formation of products is proposed as shown Figure S2: A higher temperature condition tends to trigger a homogeneous process for the hydrolysis of siloxane precursors and the following pyrolysis yields contracted microspheres with collapsed surface pores, diminishing both particle size and porosity;

at lower temperature, however, the mixture solution undergoes a phase separation between H₂O and immiscible siloxane precursors, and hydrolysis is more likely to occur at the aqueous–organic interfaces. This leads to hollow microspheres with a well-defined hierarchical nanostructure. The latter remarkably improves the permeability and accessibility of gaseous analytes to the encapsulated dye molecules in the organosilica hosts and is preferable in gas sensing applications.

3.4. Limit of Detection and Specificity

As an approach for quantitative determination of cyclohexanone, the response curve of the more responsive sensor (i.e., microspheres obtained at 150 °C) is plotted to demonstrate the correlation of sensor responses as a function of the concentration (Figure 7). The calibration curve shows good linearity in the low concentration range of 0.1–2.5 ppm, from which the limit of detection (LOD) can be calculated by extrapolating the curve to the concentration where the signal is equal to three times as much as the noise (i.e., $S/N = 3$). An estimated LOD of ~0.15 ppm was achieved based on 2 min of exposure, which was well below the vapor pressure of cyclohexanone, which was ~6500 ppm at 20 °C.

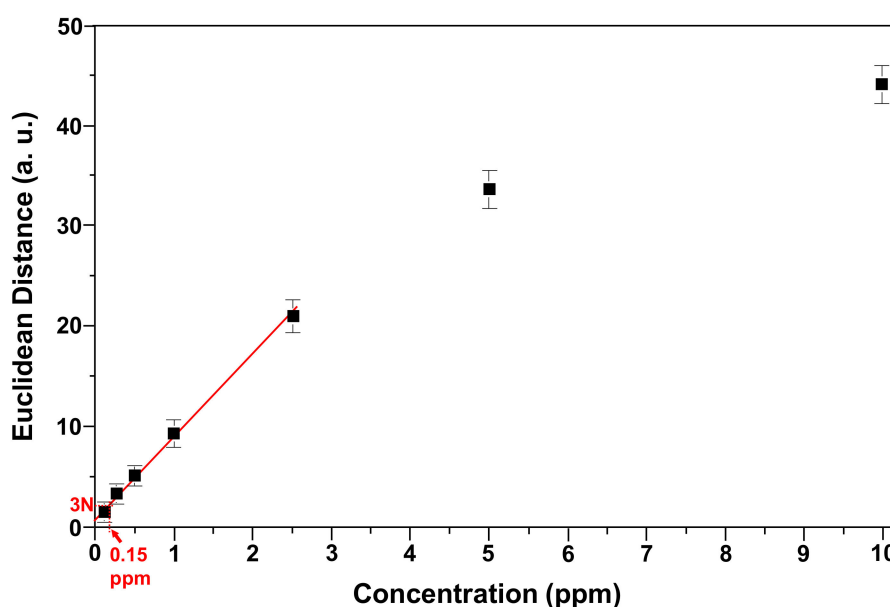


Figure 7. The calculation of the limit of detection of cyclohexanone. Data points between 0.1 and 2.5 ppm were linearly fitted and extrapolated to the concentration when signal-to-noise ratio ($S/N = 3$). The limit of detection (LOD) is estimated to be ~0.15 ppm.

The paper-based colorimetric sensor strip, reported herein, is ideal for the rapid headspace inspection of unknown samples in the field and superior to prior studies on cyclohexanone detection, in terms of the sensitivity. In comparison with the functionalized single-walled carbon nanotube (SWCNT)-based chemiresistors, developed by Swager et al. [52] for similar applications, the current method was able to substantially improve LOD from 5 ppm to low sub-ppm level by slightly elongating the exposure time from 30 s to 2 min. Compared to the recent results of optical cyclohexanone sensing, using the same colorimetric probe but different host matrices (i.e., plasticized films, with neither significant microscale structure nor comparable surface areas), sensor response from organosilica microspheres was generally 30–50% higher for each concentration, and the reported sensitivity in current work was enhanced 4–5 times (0.15 ppm vs. 0.84 ppm) [53]. This demonstrates the primary role of the hierarchical nanostructure in improving optical properties of sensing materials.

Measurements of various interferents with or without the presence of real analytes were performed to demonstrate the chemical selectivity of the developed optical sensor. A very small response in the sensor to changes in humidity was actually observed (Figure S3): Sensor response is nearly

at the same level as the controls for the exposure of 1 ppm cyclohexanone at a RH ranging from 10–90%. This is in large part due to the use of hydrophobic formulations to prevent the potential contact of water molecules with sensor elements. I further tested the sensor against a series of organic solvents that can be commonly found in the household environment or during the manufacturing of explosives. The sensor is designed to primarily probe the electrophilic property of targeted ketone species, and, therefore, it ought to be less responsive to other classes of volatile organic compounds. In accord with this expectation, the sensor exhibited ideal chemical specificity toward cyclohexanone: A very tiny response was observed for the exposure of ethanol, acetonitrile, ether, ammonia and ethyl acetate (Figure 8). Tests of potential interferents illustrate the possible applications of the developed sensor for field screening of explosives that could contain trace amount of cyclohexanone as characteristic impurities.

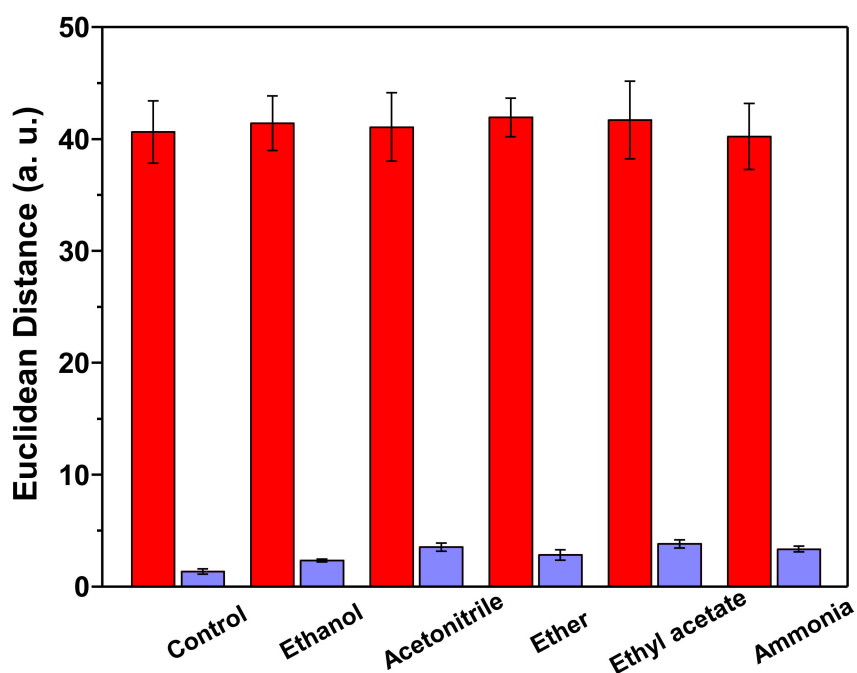


Figure 8. Sensor responses to 1 ppm cyclohexanone with (red bars) or without (blue bars) the presence of interferents, all at 1 ppm. Error bars showing the standard deviation among three replicates of each analyte are displayed.

4. Conclusions

A new method that encapsulates a chemo-responsive dye in highly porous organosilica matrices was reported for sensitive colorimetric detection of trace amounts of cyclohexanone, a volatile explosive indicator from nitro-compounds, such as RDX and HMX. Using ultrasonic and aerosol-gel synthesis, hierarchically nanoporous microspheres were produced at relatively low temperature as colorimetric sensor inks. Silica-dye composite microspheres had an average diameter of ~500 nm, with the size of nanopores being around 1–2 nm. The paper-based colorimetric sensor strip allowed for the quick quantification of gaseous cyclohexanone in 2 min, with a detection limit down to ~150 ppb. The silica-dye composite sensor was optically responsive to cyclohexanone but insensitive to common interferents involved in the production of nitro-explosives, including humidity, ethanol, acetonitrile, ether, ethyl acetate and ammonium hydroxide. The continuous and scalable ultrasonic spray synthesis provides a facile approach to prepare porous materials with hierarchical nanostructures for the ultrasensitive detection of gas analytes. This method has significant implications in the detection and identification of non-volatile nitro-explosives via the recognition of signature molecules from the

headspace gas, and may pave a path for developing a useful complement to other available sensing technologies used in security checks and forensic assessment of improvised explosives.

Supplementary Materials: The following are available online at <http://www.mdpi.com/2227-9040/6/3/34/s1>, Figure S1: Powder XRD patterns of two silica-dye microspheres synthesized at 150 and 300 °C. The spectra confirm the amorphous structures of both microspheres. Figure S2: Proposed mechanisms showing the formation of porous microspheres at (a) 150 and (b) 300 °C. Figure S3: Humidity tests of microsphere-based sensors synthesized at 150 °C. (a) Before- and after-exposure images of the sensor spot and RGB difference profiles upon exposure of 1 ppm cyclohexanone with the 10–90% relative humidity (RH), which is displayed in the color range of 3–10. (b) Sensor response to 1 ppm cyclohexanone at different levels of RH.

Acknowledgments: Z.L. acknowledges the postdoctoral financial support from the Procter & Gamble Foundation (085310). This work was carried out in part in the Frederick Seitz Materials Research Laboratory Central Facilities at the University of Illinois and the Analytical Instrumentation Facility (AIF) at the North Carolina State University.

Conflicts of Interest: The author declares no conflict of interest.

References

1. Yinon, J. *Counterterrorist Detection Techniques of Explosives*; Elsevier: Amsterdam, The Netherlands, 2007.
2. Strobbia, P.; Odion, R.; Vo-Dinh, T. Spectroscopic chemical sensing and imaging: From plants to animals and humans. *Chemosensors* **2018**, *6*, 11. [[CrossRef](#)]
3. Long, Y.; Chen, J. Systematic study of the reaction kinetics for HMX. *J. Phys. Chem. A* **2015**, *119*, 4073–4082. [[CrossRef](#)] [[PubMed](#)]
4. Chatterjee, S.; Deb, U.; Datta, S.; Walther, C.; Gupta, D.K. Common explosives (TNT, RDX, HMX) and their fate in the environment: Emphasizing bioremediation. *Chemosphere* **2017**, *184*, 438–451. [[CrossRef](#)] [[PubMed](#)]
5. Lai, H.; Leung, A.; Magee, M.; Almirall, J.R. Identification of volatile chemical signatures from plastic explosives by SPME-GC/MS and detection by ion mobility spectrometry. *Anal. Bioanal. Chem.* **2010**, *396*, 2997–3007. [[CrossRef](#)] [[PubMed](#)]
6. Chen, G.; Xia, M.; Lei, W.; Wang, F.; Gong, X. Prediction of crystal morphology of cyclotrimethylene trinitramine in the solvent medium by computer simulation: A case of cyclohexanone solvent. *J. Phys. Chem. A* **2014**, *118*, 11471–11478. [[CrossRef](#)] [[PubMed](#)]
7. Ong, T.-H.; Mendum, T.; Geurtsen, G.; Kelley, J.; Ostrinskaya, A.; Kunz, R. Use of mass spectrometric vapor analysis to improve canine explosive detection efficiency. *Anal. Chem.* **2017**, *89*, 6482–6490. [[CrossRef](#)] [[PubMed](#)]
8. Rahman, M.M.; Jiang, T.; Tang, Y.; Xu, W. A simple desorption atmospheric pressure chemical ionization method for enhanced non-volatile sample analysis. *Anal. Chim. Acta* **2018**, *1002*, 62–69. [[CrossRef](#)] [[PubMed](#)]
9. Zamora, D.; Amo-Gonzalez, M.; Lanza, M.; Fernández de la Mora, G.; Fernández de la Mora, J. Reaching a vapor sensitivity of 0.01 parts per quadrillion in the screening of large volume freight. *Anal. Chem.* **2018**, *90*, 2468–2474. [[CrossRef](#)] [[PubMed](#)]
10. Stefanuto, P.-H.; Perrault, K.; Focant, J.-F.; Forbes, S. Fast chromatographic method for explosive profiling. *Chromatography* **2015**, *2*, 213–224. [[CrossRef](#)]
11. Strle, D.; Štefane, B.; Trifkovič, M.; Van Miden, M.; Kvasić, I.; Zupanič, E.; Mušević, I. Chemical selectivity and sensitivity of a 16-channel electronic nose for trace vapour detection. *Sensors* **2017**, *17*, 2845. [[CrossRef](#)] [[PubMed](#)]
12. Patil, S.J.; Duragkar, N.; Rao, V.R. An ultra-sensitive piezoresistive polymer nano-composite microcantilever sensor electronic nose platform for explosive vapor detection. *Sens. Actuators B Chem.* **2014**, *192*, 444–451. [[CrossRef](#)]
13. Li, Z.; Bassett, W.P.; Askim, J.R.; Suslick, K.S. Differentiation among peroxide explosives with an optoelectronic nose. *Chem. Commun.* **2015**, *51*, 15312–15315. [[CrossRef](#)] [[PubMed](#)]
14. Staymates, M.E.; MacCrehan, W.A.; Staymates, J.L.; Kunz, R.R.; Mendum, T.; Ong, T.-H.; Geurtsen, G.; Gillen, G.J.; Craven, B.A. Biomimetic sniffing improves the detection performance of a 3D printed nose of a dog and a commercial trace vapor detector. *Sci. Rep.* **2016**, *6*, 36876. [[CrossRef](#)] [[PubMed](#)]
15. Roscioli, K.M.; Davis, E.; Siems, W.F.; Mariano, A.; Su, W.; Guharay, S.K.; Hill, H.H. Modular ion mobility spectrometer for explosives detection using corona ionization. *Anal. Chem.* **2011**, *83*, 5965–5971. [[CrossRef](#)] [[PubMed](#)]

16. Senesac, L.; Thundat, T.G. Nanosensors for trace explosive detection. *Mater. Today* **2008**, *11*, 28–36. [[CrossRef](#)]
17. Peng, L.; Hua, L.; Wang, W.; Zhou, Q.; Li, H. On-site rapid detection of trace non-volatile inorganic explosives by stand-alone ion mobility spectrometry via acid-enhanced evaporation. *Sci. Rep.* **2014**, *4*, 6631. [[CrossRef](#)] [[PubMed](#)]
18. Choi, S.-S.; Son, C.E. Analytical method for the estimation of transfer and detection efficiencies of solid state explosives using ion mobility spectrometry and smear matrix. *Anal. Methods* **2017**, *9*, 2505–2510. [[CrossRef](#)]
19. Mujahid, A.; Dickert, F. Surface acoustic wave (SAW) for chemical sensing applications of recognition layers. *Sensors* **2017**, *17*, 2716. [[CrossRef](#)] [[PubMed](#)]
20. Gupta, D.; Chen, X.; Wang, C.-C.; Trivedi, S.; Choa, F.-S. Stand-off chemical detection using photoacoustic sensing techniques—From single element to phase array. *Chemosensors* **2018**, *6*, 6. [[CrossRef](#)]
21. Nimal, A.T.; Mittal, U.; Singh, M.; Khaneja, M.; Kannan, G.K.; Kapoor, J.C.; Dubey, V.; Gutch, P.K.; Lal, G.; Vyas, K.D.; et al. Development of handheld SAW vapor sensors for explosives and CW agents. *Sens. Actuators B Chem.* **2009**, *135*, 399–410. [[CrossRef](#)]
22. García-Calvo, J.; Calvo-Gredilla, P.; Ibáñez-Llorente, M.; Romero, D.C.; Cuevas, J.V.; García-Herbosa, G.; Avella, M.; Torroba, T. Surface functionalized silica nanoparticles for the off-on fluorogenic detection of an improvised explosive, tntp, in a vapour flow. *J. Mater. Chem. A* **2018**, *6*, 4416–4423. [[CrossRef](#)]
23. Chen, H.-Y.; Ruan, L.-W.; Jiang, X.; Qiu, L.-G. Trace detection of nitro aromatic explosives by highly fluorescent g-C₃N₄ nanosheets. *Analyst* **2015**, *140*, 637–643. [[CrossRef](#)] [[PubMed](#)]
24. Peng, X.; Liu, H.; Liu, A.; Xu, W.; Fu, Y.; He, Q.; Cao, H.; Cheng, J. Ultrasensitive and direct fluorescence detection of RDX explosive vapor via side-chain terminal functionalization of a polyfluorene probe. *Anal. Methods* **2018**, *10*, 1695–1702. [[CrossRef](#)]
25. Wang, C.; Huang, H.; Bunes, B.R.; Wu, N.; Xu, M.; Yang, X.; Yu, L.; Zang, L. Trace detection of RDX, HMX and PETN explosives using a fluorescence spot sensor. *Sci. Rep.* **2016**, *6*, 25015. [[CrossRef](#)] [[PubMed](#)]
26. Malik, A.K.; Rai, P.K. Development of a new SPME–HPLC–UV method for the analysis of nitro explosives on reverse phase amide column and application to analysis of aqueous samples. *J. Hazard. Mater.* **2009**, *172*, 1652–1658.
27. Bianchi, F.; Bedini, A.; Riboni, N.; Pinalli, R.; Gregori, A.; Sidisky, L.; Dalcanale, E.; Careri, M. Cavitand-based solid-phase microextraction coating for the selective detection of nitroaromatic explosives in air and soil. *Anal. Chem.* **2014**, *86*, 10646–10652. [[CrossRef](#)] [[PubMed](#)]
28. McEneff, G.L.; Murphy, B.; Webb, T.; Wood, D.; Irlam, R.; Mills, J.; Green, D.; Barron, L.P. Sorbent film-coated passive samplers for explosives vapour detection part A: Materials optimisation and integration with analytical technologies. *Sci. Rep.* **2018**, *8*, 5815. [[CrossRef](#)] [[PubMed](#)]
29. Albert, K.J.; Lewis, N.S.; Schauer, C.L.; Sotzing, G.A.; Stitzel, S.E.; Vaid, T.P.; Walt, D.R. Cross-reactive chemical sensor arrays. *Chem. Rev.* **2000**, *100*, 2595–2626. [[CrossRef](#)] [[PubMed](#)]
30. Li, Z.; Suslick, K.S. Ultrasonic preparation of porous silica-dye microspheres: Sensors for quantification of urinary trimethylamine N-oxide. *ACS Appl. Mater. Interfaces* **2018**, *10*, 15820–15828. [[CrossRef](#)] [[PubMed](#)]
31. Askim, J.R.; Li, Z.; LaGasse, M.K.; Rankin, J.M.; Suslick, K.S. An optoelectronic nose for identification of explosives. *Chem. Sci.* **2016**, *7*, 199–206. [[CrossRef](#)] [[PubMed](#)]
32. Li, Z.; Li, H.; LaGasse, M.K.; Suslick, K.S. Rapid quantification of trimethylamine. *Anal. Chem.* **2016**, *88*, 5615–5620. [[CrossRef](#)] [[PubMed](#)]
33. Li, Z.; Jang, M.; Askim, J.R.; Suslick, K.S. Identification of accelerants, fuels and post-combustion residues using a colorimetric sensor array. *Analyst* **2015**, *140*, 5929–5935. [[CrossRef](#)] [[PubMed](#)]
34. Nery, E.W.; Kubota, L.T. Sensing approaches on paper-based devices: A review. *Anal. Bioanal. Chem.* **2013**, *405*, 7573–7595. [[CrossRef](#)] [[PubMed](#)]
35. Li, Z.; Suslick, K.S. Portable optoelectronic nose for monitoring meat freshness. *ACS Sens.* **2016**, *1*, 1330–1335. [[CrossRef](#)]
36. Khodasevych, I.; Parmar, S.; Troynikov, O. Flexible sensors for pressure therapy: Effect of substrate curvature and stiffness on sensor performance. *Sensors* **2017**, *17*, 2399. [[CrossRef](#)] [[PubMed](#)]
37. Burleigh, M.C.; Markowitz, M.A.; Spector, M.S.; Gaber, B.P. Porous organosilicas: An acid-catalyzed approach. *Langmuir* **2001**, *17*, 7923–7928. [[CrossRef](#)]

38. Ma, M.; Yan, F.; Yao, M.; Wei, Z.; Zhou, D.; Yao, H.; Zheng, H.; Chen, H.; Shi, J. Template-free synthesis of hollow/porous organosilica-Fe₃O₄ hybrid nanocapsules toward magnetic resonance imaging-guided high-intensity focused ultrasound therapy. *ACS Appl. Mater. Interfaces* **2016**, *8*, 29986–29996. [[CrossRef](#)] [[PubMed](#)]
39. Du, G.; Peng, J.; Zhang, Y.; Zhang, H.; Lü, J.; Fang, Y. One-step synthesis of hydrophobic multicompartiment organosilica microspheres with highly interconnected macro-mesopores for the stabilization of liquid marbles with excellent catalysis. *Langmuir* **2017**, *33*, 5223–5235. [[CrossRef](#)] [[PubMed](#)]
40. Qiang, Z.; Guo, Y.; Liu, H.; Cheng, S.Z.D.; Cakmak, M.; Cavicchi, K.A.; Vogt, B.D. Large-scale roll-to-roll fabrication of ordered mesoporous materials using resol-assisted cooperative assembly. *ACS Appl. Mater. Interfaces* **2015**, *7*, 4306–4310. [[CrossRef](#)] [[PubMed](#)]
41. Skrabalak, S.E.; Suslick, K.S. Porous MoS₂ synthesized by ultrasonic spray pyrolysis. *JACS* **2005**, *127*, 9990–9991. [[CrossRef](#)] [[PubMed](#)]
42. Bang, J.H.; Helmich, R.J.; Suslick, K.S. Nanostructured ZnS: Ni²⁺ photocatalysts prepared by ultrasonic spray pyrolysis. *Adv. Mater.* **2008**, *20*, 2599–2603. [[CrossRef](#)]
43. Xu, H.; Zeiger, B.W.; Suslick, K.S. Sonochemical synthesis of nanomaterials. *Chem. Soc. Rev.* **2013**, *42*, 2555–2567. [[CrossRef](#)] [[PubMed](#)]
44. Jerónimo, P.C.A.; Araújo, A.N.; Montenegro, M.C.B.S.M. Optical sensors and biosensors based on sol-gel films. *Talanta* **2007**, *72*, 13–27.
45. Yao, N.; Xiong, G.; Yeung, K.L.; Sheng, S.; He, M.; Yang, W.; Liu, X.; Bao, X. Ultrasonic synthesis of silica-alumina nanomaterials with controlled mesopore distribution without using surfactants. *Langmuir* **2002**, *18*, 4111–4117. [[CrossRef](#)]
46. Roy, B.; Halder, S.; Guha, A.; Bandyopadhyay, S. Highly selective sub-ppm naked-eye detection of hydrazine with conjugated-1,3-diketo probes: Imaging hydrazine in *Drosophila* larvae. *Anal. Chem.* **2017**, *89*, 10625–10636. [[CrossRef](#)] [[PubMed](#)]
47. Xiao, L.; Tu, J.; Sun, S.; Pei, Z.; Pei, Y.; Pang, Y.; Xu, Y. A fluorescent probe for hydrazine and its in vivo applications. *RSC Adv.* **2014**, *4*, 41807–41811. [[CrossRef](#)]
48. Baud, D.; Ladkau, N.; Moody, T.S.; Ward, J.M.; Hailes, H.C. A rapid, sensitive colorimetric assay for the high-throughput screening of transaminases in liquid or solid-phase. *Chem. Commun.* **2015**, *51*, 17225–17228. [[CrossRef](#)] [[PubMed](#)]
49. Dilek, O.; Bane, S. Turn on fluorescent probes for selective targeting of aldehydes. *Chemosensors* **2016**, *4*, 5. [[CrossRef](#)]
50. Li, Z.; Suslick, K.S. A hand-held optoelectronic nose for the identification of liquors. *ACS Sens.* **2018**, *3*, 121–127. [[CrossRef](#)] [[PubMed](#)]
51. Barrett, E.P.; Joyner, L.G.; Halenda, P.P. The determination of pore volume and area distributions in porous substances. I. Computations from nitrogen isotherms. *JACS* **1951**, *73*, 373–380. [[CrossRef](#)]
52. Frazier, K.M.; Swager, T.M. Robust cyclohexanone selective chemiresistors based on single-walled carbon nanotubes. *Anal. Chem.* **2013**, *85*, 7154–7158. [[CrossRef](#)] [[PubMed](#)]
53. Li, Z.; Fang, M.; LaGasse, M.K.; Askim, J.R.; Suslick, K.S. Colorimetric recognition of aldehydes and ketones. *Angew. Chem. Int. Ed.* **2017**, *56*, 9860–9863. [[CrossRef](#)] [[PubMed](#)]

